ISSN 1087-6596, Glass Physics and Chemistry, 2015, Vol. 41, No. 3, pp. 307–315. © Pleiades Publishing, Ltd., 2015.

Generation and Collapse of Bubbles in Lead Silicate Glass[1]

Rafi Ali Rahimi[a] and S. K. Sadrnezhaad[b]

[a] *Material Research School, Nuclear Science and Technology Research Institute (NSTRI), Atomic Energy Organization of Iran, P.O. Box 81465-1589, Esfahan, Iran*

[b] *Department of Materials Science and Engineering, Sharif University of Technology, P.O. Box 11365-9466, Tehran, Iran*

e-mail: sadrnezh@sharif.edu

Received July 25, 2013

Abstract—Presence of bubbles affects quality of the lead silicate glass (LSG) samples. This paper presents the most recent results obtained on formation and collapse of bubbles in LSG melts. Main sources of the bubbles are dissolved gases and redox reactions. A foamy layer full of bubbles rapidly forms at top of the molten phase. Effect of viscosity and density of the melt on content and ascension rate of the bubbles are investigated. Number and mean diameter of the bubbles and thickness of the top bubbly layer are calculated from gas volume measurements and image analysis via J software.

Keywords: amorphous materials, glasses, optical materials, oxides, defects

DOI: 10.1134/S1087659615030128

INTRODUCTION

Reaction of silica with the neighboring constituents present in the glass melting system results in formation and dispersion of so many bubbles in the highly-viscous molten phase. Quality of the produced glass deteriorates if all bubbles together with unmelted silica particles are trapped into the solidified phase. Such imperfections negatively affect economics of the glass melting system [1, 2]. Extensive mathematical studies have been done on removal of gas bubbles from glass-melts under different conditions by previous authors [3, 4].

Air which comes with the raw-materials and gases (CO_2, SO_2 and O_2) which form by decomposition of the initial constituents (carbonates, sulfates, ...) and chemical reactions between them may dissolve in the liquid phase [5–7]. Above saturation level, the pressure difference ΔP between non-equilibrium and equilibrium states creates a driving force for new bubble formation. A fraction of the pressure difference $f\Delta P$ (f is the fraction coefcient) is consumed by bubble creation and the remaining $(1-f)\Delta P$ is spent by viscous dissipation in the melt. Considering $f\Delta P$ as a potential for bubble creation (energy per unit volume), standard nucleation kinetics can be utilized to predict the bubble formation rate. This enables us to represent the free energy ΔG for bubble nucleation by the expression [8–12]:

$$\Delta G = -\frac{4}{3}\pi r^3 f \cdot \Delta P + 4\pi r^2 \sigma, \qquad (1)$$

where r is the bubble radius and σ is the glassy melt-gas interfacial tension.

Previous investigators have studied nucleation, growth and ascension of bubbles through different melts [5–9, 13]. Nucleation and growth of CH_4 in water have been studied by Ho-Young Kwak [8]. They did not observe bubble nucleation at pressures between 1 and 68 atmospheres because this was lower than the decompression pressure needed for spontaneous bubble nucleation of the methane (~120 atm). Bubble nucleation was activated, however, when shear flow was applied from 1 to 5 min after the decompression. Nadav G. Lensky [9] has performed experiments on CO_2 bubble nucleation inside saturated basalt melt under 1.5 GPa and 1350°C. It has been found that the decompression more than 300 MPa is needed for initiation of the bubble nucleation.

Nemec [5, 6] has studied refining mechanism of soda-lime-silica glass melt which contains bubbles. Heterogeneous bubble nucleation has been concluded from the experimental and theoretical studies. Bubble growth and ascension are the most important mechanisms accelerating refining of glass melt. The role of refining agents is rather complex influencing both the velocity of bubble ascension and the velocity of the sands dissolution. In soda-lime-silica glass melting process the refining reactions take place in temperatures beyond 1100°C. Thus, if the batch reaches temperatures larger than 1100°C it undergoes two consecutive expansions: the first one is due to CO_2 release, and the second is due to generation of refining gases. Note that in the carbon-containing batch, carbon dioxide partly reacts with carbon-containing compo-

[1] The article is published in the original.

Chemical composition of lead silicate glass

Glass sample	Composition, wt %								
	PbO	SiO_2	CaO	ZrO_2	TiO_2	MgO	Alkaline (Na, K)	As_2O_3	Al_2O_3
LSG	68.5	24	–	2.4	1	–	1.6	0.3	2.2
Window glass	–	73	9	–	–	4	14	–	–

nents to generate carbon monoxide CO at the temperatures above 750°C. The latter becomes entrapped in the batch and can react with sodium sulfate (refining agent) to form SO_2 gas causing further batch expansion [14]. In such cases due to very high super saturation, the large number of bubbles is formed.

Different mechanisms dominate dynamics of the foam formation during different stages of the process. Foam formation is depending on the balance between the bubble built-up in the foam due to gas influx and the flowing of liquid from the channels between the bubbles. In the early stages of the process, the influx of gas molecules is high and the thickness of the foamy layer is growing. In the latter stage of the process, when the foam is sufficiently drained and the lamellae separating bubbles in the foam become thin, the bubble coalescence and inter bubble gas diffusion tend to become dominant at least at the top of the foam [15, 16].

Information about kinetics of bubble removing process can effectively help synthesis of high lead content silicate glasses. The main objective of this work is studying about the source of the gas molecules creating bubbles and also on behavior of bubbles in lead silicate melt at its melting temperature and investigation of kinetics of bubble removal. Number and volume of bubbles were estimated by measuring diameter of various bubbles using Image J software [17], optical image analysis and volume evaluation from density measurement. Main factors affecting removal of bubbles accumulated at the surface of the lead silicate glass (LSG) melt were determined.

EXPERIMENTAL PROCEDURE

LSG was produced from technical grade silica (SiO_2 > 99.9%, Hamedan, Iran), red lead (Pb_3O_4 > 99%, Iran) and reagent grade Na_2O, K_2O, ZrO_2, TiO_2 and As_2O_3 (Aldrich Chemical Co.) powders. Molten soda-lime-silica glass was also prepared by melting ordinary window glass powders at 1400°C. The chemical composition of both glasses is given in table. The behavior of bubbles in this glass was compared with LSG samples. Batch of mixed materials of LSG weighing 500 g were charged into alumina crucibles and heated with electric furnace (Exciton Co., Iran). The temperature was set at 1300°C for 2 h under 1 atmosphere and then the melt was quenched in water for achievement of acceptable homogeneity. The produced frit was wet ground to <200 grit. Ground powder was dried in an oven at 110°C and was heated to 1200°C. The quenching, grinding and melting of LSG was twice repeated.

In order to estimate the volume of bubbles inside glass melt, we devised a method for measuring the density of glass containing gas bubbles. Volume change due to reaction of alumina crucible with the lead silicate glass melt was assumed negligible. Using Image J software [17], the diameter of bubbles was determined from optical images of the LSG melt. Then the number of bubbles in each sample was calculated from their mean diameter.

Weights of crucibles (dry, wet, loaded, unloaded and buoyancy affected) were measured before and after melting of the glass sample by Mettler Toledo AG204 electric balance having accuracy of ±0.0001 g. Different batches of lead silicate glass powder weighing 50 g were poured into these alumina crucibles and heated in electric furnace (Exciton Co., Iran) and were separately held at 900, 950, 1000, 1050 and 1100°C for 15, 30 and 45 min. The furnace was subsequently turned off and slowly cooled down to the room temperature.

Apparent density of the crucibles with glass inside them was calculated from the following relation [18]:

$$d = \frac{W_d}{W_d - W_b}, \quad (2)$$

where d is the apparent density, W_d is the dry and W_b is the buoyancy affected weight of the glass with crucible. By specifying the apparent density of each crucible with and without glass, the density of glass was calculated by the following relation [19]:

$$D_t = D_g V_g + D_c V_c, \quad (3)$$

where D is density and V is volume fraction, subscripts t, g and c stand for total, glass and crucible.

Glass inside crucible contains two parts: a top bubbly layer and a bottom part without bubble. The total weight of glass inside each crucible (bubbly glass and a glassy layer without bubble) was 50 g and then the total volume of glass (with and without bubble) in each crucible was determined from the following relation:

$$V_{g\text{–total}} = \frac{W_{g\text{–total}}}{d_{g\text{–total}}}. \quad (4)$$

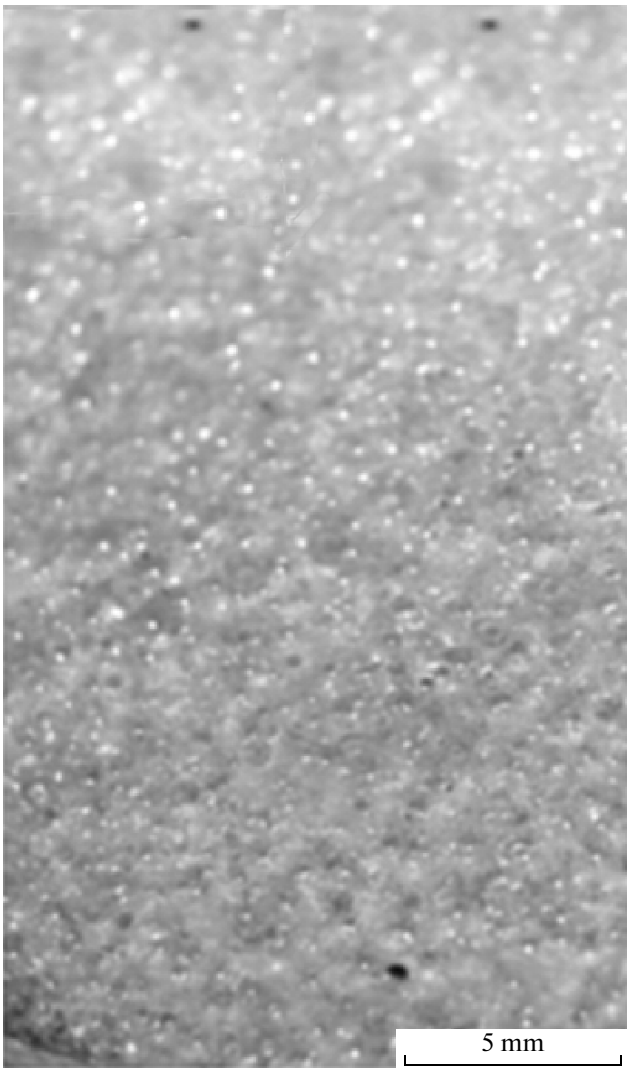

Fig. 1. Images from the lateral cross-section of the bubbly layer of LSG sample which heat treated at 900°C for 30 min.

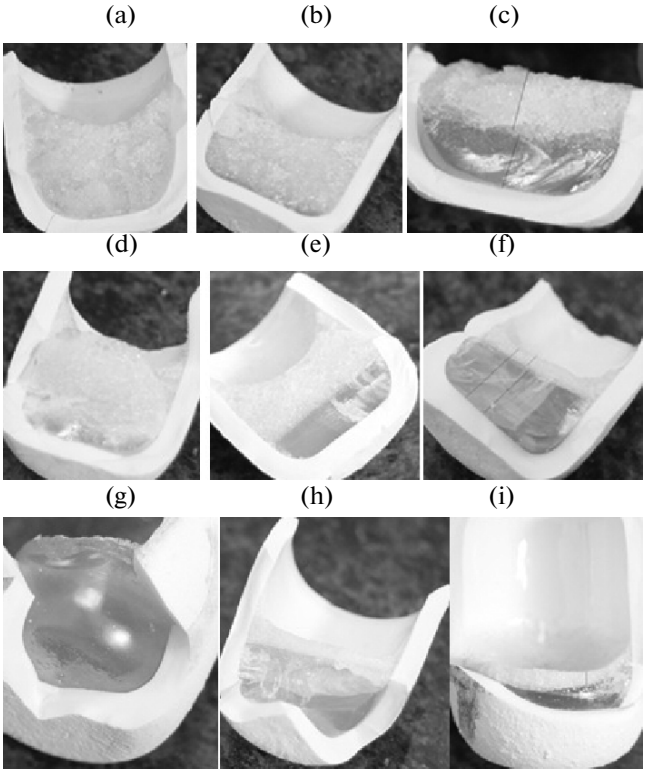

Fig. 2. Images taken from the lateral cross-section of the LSG inside alumina crucibles heat treated at 900°C for: (a) 15 min, (b) 30 min and (c) 45 min; at 950°C for: (d) 15 min; at 1000°C for: (e) 15 min, (f) 30 min and (g) 45 min; at 1050°C for: (h) 15 min; at 1100°C for: (i) 15 min.

The volume of glass without bubble was revealed by dividing the total weight of glass inside the crucible to the density of glass without bubble (containing glassy layer without bubbles and glassy layers between different bubbles in bubbly glassy layer as indicated in Figs. 1, 2 and 3, 4):

$$V_{g-\text{without bubble}} = \frac{W_{g-\text{total}}}{d_{g-\text{without bubble}}}, \quad (5)$$

where $W_{g\text{-total}}$ is the total weight of glass, $d_{g\text{-without bubble}}$ is density of nonporous glass and $V_{g\text{-without bubble}}$ is the total volume of glass without bubbles. The total volume occupied by glass inside the crucible consists of volume of glass in bubble-less layer and in layer with bubbles and the volume of the gases entrapped by the bubbles. The entrapped gas volume of each crucible was ascertained by decreasing the volume of glass without bubble from the total occupied volume of the crucible:

$$V_{\text{bubble}} = V_{g-\text{total}} - V_{g-\text{without bubble}}. \quad (6)$$

Optical images taken from surface and cross section of the bubbly region (Figs. 1, 2 and 3, 4) indicate accumulation of the bubbles at the upper part of the melt. From these images, sizes of bubbles are estimated by using Image J software. The mean bubble sizes were determined by measuring the diameter of several bubbles in 1 cm^2 area and taking the average

$$\overline{X} = \frac{\sum X_i}{n}. \quad (7)$$

Size average and standard deviations of the bubbles were calculated by using the following relations:

$$\delta = \frac{1}{n}\sum \left|X_i - \overline{X}\right|, \quad (8)$$

$$\delta_m = \frac{\sqrt{\sum (X_i - \overline{X})^2}}{\sqrt{n(n-1)}}, \quad (9)$$

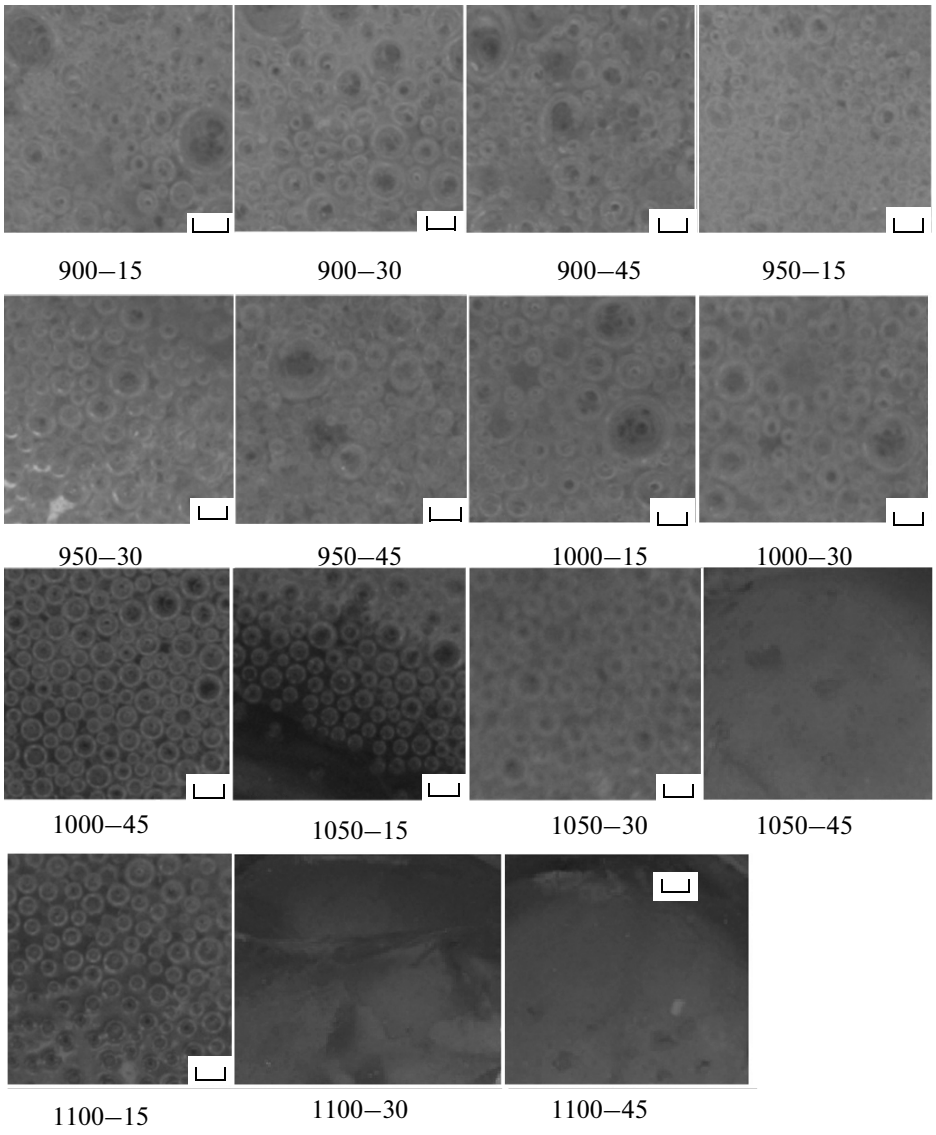

Fig. 3. Images of bubbles on the surface of the samples which heat treated at different time and temperature conditions. The line scale shown on the surface of the images indicates 1 mm length.

where X_i is bubble diameter, $\overline{X}$ is mean bubble diameter and n is the total number of bubbles in measured area.

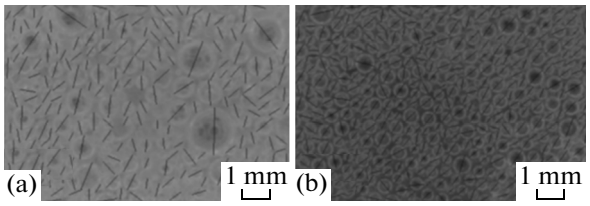

Fig. 4. Images taken from the surface of the samples showing method of measuring the diameter of bubbles by using Image J software.

The number of bubbles in each sample is determined by dividing the total volume of gas bubbles to the mean volume for each bubble:

$$N = \frac{V_{\text{total bubbles}}}{V_{\text{mean for each bubble}}} \quad (10)$$

Reduction in thickness or number of bubbles in the bubbly layer was used to determine kinetics of the bubble removing process. The samples were cut by a diamond hacksaw and their thickness was measured by a clipper. Image J software was also used to determine sizes of the bubbles from the section images. The thicknesses obtained from two methods were consistent.

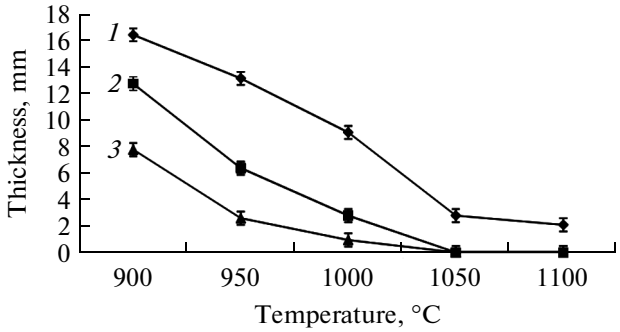

Fig. 5. Variation of bubbly layer thickness in samples heat treated at different time (min) 15 (*1*), 30 (*2*), 45 (*3*) and temperature conditions.

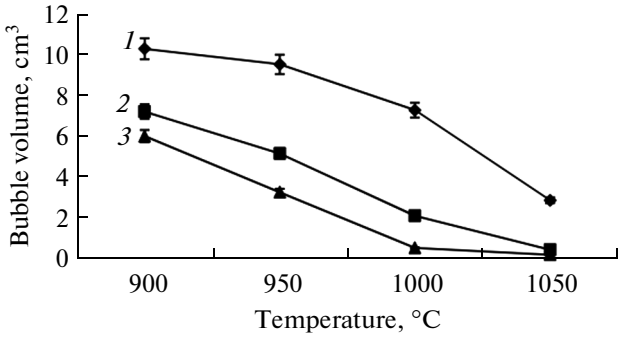

Fig. 6. Variation of the volume of bubbles in samples heat treated at different time (min) and temperature conditions.

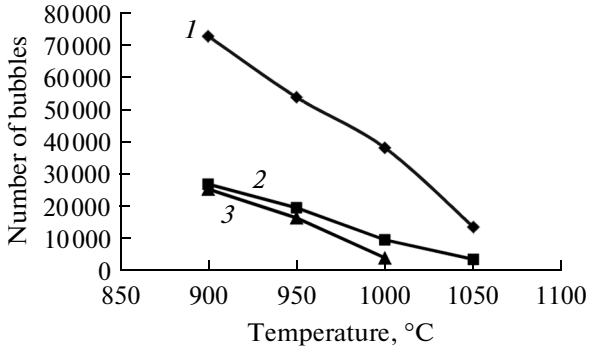

Fig. 7. Variation of the number of bubbles from the surface of the samples heat treated at different time (min): 10 (*1*), 30 (*2*), 45 (*3*) and temperature conditions.

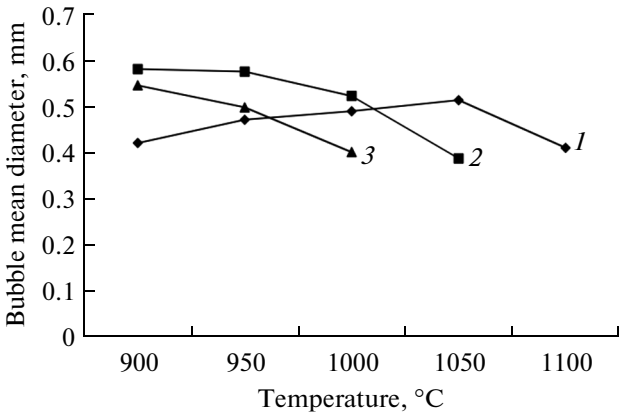

Fig. 8. The variation of mean bubble size with heat treatment temperatures and time (min): 15 (*1*), 30 (*2*), 45 (*3*).

RESULTS

Figure 1 shows an image from the depth profile of the bubbly layer of LSG sample. The upper section is faint-colored but the lower section is stronger in color. This indicates that the thickness of the glassy lamella between bubbles in the lower section is thicker than from the upper section and also the size distribution of the bubbles in depth is the same as in the surface of the melt. Figure 2 shows the images of the lateral sections of LSG solidified inside alumina crucible (*a* to *c*) and solid soda-lime-silica glass without crucible (*d*). It shows three cases of (*a*) full bubbly, (*b*) bubbly and (*c*) bubble less in the lead silicate glass. In partial bubbly case they have been accumulated on the surface of the LSG melt.

Effects of heat treating in 900, 950, 1000, 1050 and 1100°C temperatures for 15, 30 and 45 min on bubble formation in the LSG melt are shown in Figs. 5 to 7. These figures illustrate bubbly layer thickness (Fig. 5), bubble volume (Fig. 6) and number of bubbles (Fig. 7) versus heating temperature at different times. The bubbly layer thickness becomes zero in samples which are maintained at 1050°C for 30 and 45 min; but a bubbly layer still exists in samples maintained for 15 min at 1100°C. The bubbles have large volume at 900°C for 15 min (Fig. 6). The amount of large bubbles reduces by increasing temperature and time. The number of bubbles strictly reduces by increase of holding time from 15 to 30 min (Fig. 7), but its reduction rate is reduced by increase of time from 30 to 45 min.

Figure 3 shows the images taken from the surface of the samples heat treated at different times and temperatures. It shows the size distribution of the bubbles in the different heat treatment conditions. Figure 4 shows the images taken from the surface of two different samples which heat treated at separate time and temperatures. Bubbles at this magnification are nearly obvious then their diameters measured for all samples by using Image J software. By using this statistical information, mean diameter, average and standard deviations were determined.

Figures 8, 9 and 10 show variations of mean bubble size, average and standard deviations for different samples in various heat treatment conditions. As indicated in Fig. 8, the mean bubble size is small in heat treatment condition of 15 min at 900°C. Its value

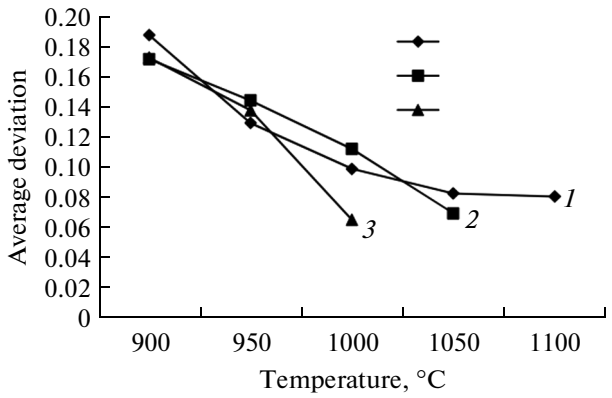

Fig. 9. The variation of deviation from average bubble size with temperature and time (min): 15 (*1*), 30 (*2*), 45 (*3*).

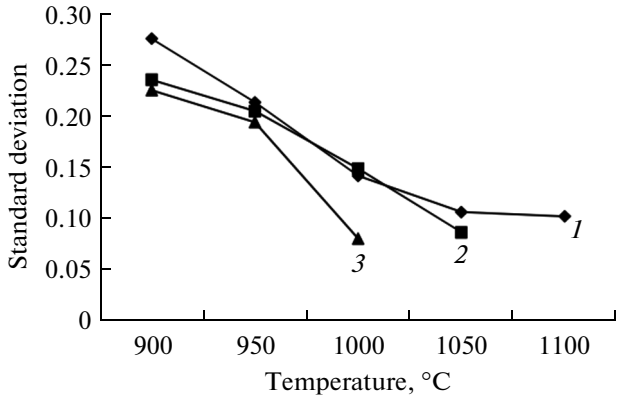

Fig. 10. The variation of standard deviation from mean bubble size with temperature and time(min): 15 (*1*), 30 (*2*), 45 (*3*).

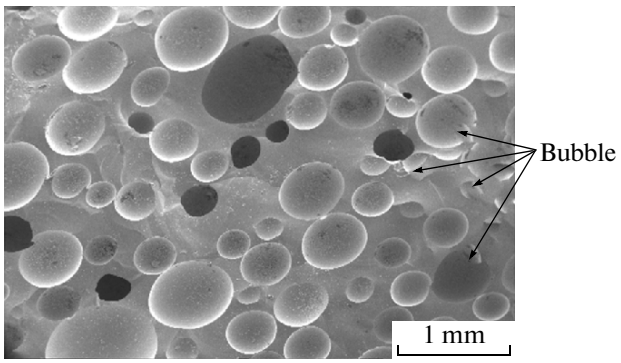

Fig. 11. SEM micrograph of the bubbles accumulated at the surface of the LSG melt.

enhances by increase of temperature to 1050°C but above this temperature it decreases. In heat treatment times of 30 and 45 min, the initial mean bubble size is high at lower temperatures and by temperature rise, they reduces. Figure 11 shows the SEM micrograph of the bubbles accumulated in the surface of the lead silicate glass melt. It confirms the size distribution of the bubbles determined by the optical images and Image J software.

DISCUSSION

Images obtained from the glassy melt indicate that a lot of bubbles form in the LSG during and after the fusion. The number of bubbles depends mostly on the surface tension, super-saturation of gas molecules and the viscosity of the melt. The surface tension and the viscosity of the lead silicate glass are relatively small. The rate of bubble nucleation and growth is, thus, large. No carbonaceous or other gas producing compounds exist in the LSG melt. Redox behavior of lead atoms is thus expected to be the source of creation of gas molecules which cause generation of foamy glass in the whole regions of the melt.

In all investigations done on PbO containing glasses, Pb^{2+}-O bond has been considered as glass modifier or glass former. There are only a few reports on glasses incorporating Pb^{4+} either in the form of PbO_2 or in the form of Pb_3O_4 [20, 21]. Pb^{4+} has not been incorporated as such, in binary or ternary glass systems, probably for the well-known dissociation tendency of PbO_2 around 290°C and (red-lead) Pb_3O_4 into yellow PbO around 550°C [22]. Among the reports on the preparation of glasses containing PbO as a constituent, Pb_3O_4 has been the starting material for in-situ generation of PbO [23].

Si^{4+} and Pb^{4+} belong to the same carbon group of the periodic table and have the same oxidation states in their dioxides. Therefore it is believed that PbO_2 partly plays the role of SiO_2 in Pb_3O_4 glass formation. The *d*-orbitals of Pb^{4+} being larger in size than the empty *d*-orbital of SiO_2, they are likely to be better employed for the propagation of the glass network. Besides SiO_2 chains in limited number and $O-Pb^{4+}-O$ links in larger proportion, the square pyramids formed by oxygen around lead (Pb^{2+}) ion probably constitute the network structure of Pb_3O_4–$xSiO_2$ glass [24].

If the lead silicate melt is cooled very slowly it is possible to have both PbO and PbO_2 mixtures at room temperature. But in quenching of lead silicate melt in cold water, the formation of Pb_3O_4 is negligible. In former stages of this process for preparing homogeneous compound, the lead silicate melt is quenched and ground to <200 grit. So kinetically it was not given any time in cooling process for changing of PbO to Pb_3O_4. But it is expected that in reheating of these fine powders, the PbO is partially changed to Pb_3O_4 by entering of oxygen molecules from the atmosphere of the furnace into the glass in temperatures lower than 550°C. In relation to the redox behavior of lead element it must be attended that in reheating of fine pow-

ders of lead silicate glass, the redox reactions are carried out in two temperature regions.

In relation to discussion of the quantity of the PbO altered to Pb_3O_4 in temperature range which the second compound is stable, the fine powders of lead silicate have so many surface areas in conjunction with the atmosphere. Then the large amount of oxygen molecules can enter to the network of this powder. It is now generally agreed that oxygen [25] diffuse as molecules in glasses. By increasing the breaking of the silicate network with higher content of network modifiers, the dis-connectivity automatically and the rate of oxygen diffusion by increasing temperature are accelerated. The oxygen molecules can react and exchange with lead elements in the glass network. Then the Pb_3O_4 modification of lead oxide is partially started to generate in lead silicate glass network.

In temperature range higher than 550°C it is dissociated to PbO and released oxygen molecules. The extraction of oxygen molecules from the surface of the lead silicate powders is concurrent with the softening of these powders and sticking of them with each other. So this phenomenon prevents from the extraction of oxygen molecules. This increases the content of dissolved oxygen molecules in the lead silicate glass and by conjunction with the dissolved air molecules trapped between the space of the powders, the dissolution of gas molecules inside viscous glassy melt reached to super saturation. Then by reaching the temperature of the melt close to 900°C, exaggerated bubble nucleation and growth is carried out.

In relation to the different non-bonding oxygen content of both LSG and soda-lime-silicate glass networks and their common refractory silica compound, their viscosities around melting temperatures differ with each others. So any discussion in relation to viscosity is in this basis. The T_g of LSG and soda-lime-silica glasses are 473 and 573°C, respectively [26]. LSG melts of lower surface energy [27] and viscosity have greater number of bubbles with lower critical radius of nucleation. The main source of bubbles in melting of raw materials of soda-lime-silica glass is the CO_2; SO_2 and oxygen molecules released from the redox reactions. When the powder of soda-lime-silica glass is melted, in this case by itself the large content of these gas molecules are eliminated. Then the critical radius of nucleation is larger and the number of bubbles is smaller because they need higher super saturation to compensate the high-viscosity and large surface tension of melt [8, 9].

For a bubble without any impurity in its boundary, the mechanical force applying to pull it to the surface of the melt is obtained from the following correlation [10]:

$$F_D = 3\pi\eta DV\left[\left(1+\frac{2\eta}{3\eta'}\right)\Big/\left(1+\frac{\eta}{\eta'}\right)\right], \quad (11)$$

where D is bubble diameter, V is ascending speed of the bubble, η is viscosity of the melt and η' is viscosity of the gases inside the bubble. Since the amount of η' is very small, then it is shortened to the following correlation [10]:

$$F_D = 2\pi\eta DV, \quad (12)$$

The governing correlation for rising velocity of the bubbles toward top of the melt is taken from the relationships pertaining to the mechanical forces affecting on the bubbles. The result was obtained by the Hadamard–Rybczynski corresponding to following correlation [28]:

$$V = 2(\rho-\rho')gD^2\left(\frac{\eta+\eta'}{2\eta+3\eta'}\Big/3\eta\right), \quad (13)$$

where ρ, η, ρ' and η' are density and viscosity of melt and gases inside the bubbles, respectively. By neglecting density and viscosity of the gases, it is abbreviated to the following correlation:

$$V = \rho g D^2/3\eta. \quad (14)$$

From the above formula, by assuming a bubble with equal diameter inside LSG or soda-lime-silica glass melt, the following relation between the rising rate of bubbles, the densities and the viscosities of the melts is obtained

$$\frac{V'}{V} = \frac{\rho'\eta}{\rho\eta'}. \quad (15)$$

The difference in bubble removing process from these glass melts is explained by the above relation. The viscosity and density of glass melt influence the bubble motion rates. The rising velocity of bubbles in various glass melts differ with each other. In Savanneh River Simulated waste glass melt by decreasing the viscosity of melt the rising velocity of bubbles are enhanced [29]. Due to higher viscosity and lower density of soda-lime-silica melt, the bubble motion and rising rate for a constant bubble diameter is very low. In LSG glass melt the rising rate of bubbles is large then this phenomenon causes formation of a bubbly layer in the surface of the melt. It seems that the bubbles are collectively moved to the surface of the melt.

In relation to Eq. (15), the higher viscosity and lower density of soda-lime-silica glass melt impedes from the rising of bubbles toward top of the melt. Then the amount of buoyancy force necessary for pulling of bubbles increases. It is obtained by growth of bubbles via penetrating of the dissolved gas molecules into the bubbles. Then it is necessary to spend higher time for growing of bubbles and reaching them to the size which the buoyancy force can pull them to the surface of the melt. Then the total time for ascension of bubbles from soda-lime-silica glass may be many times larger than the time needed for bubble ascension in LSG melt. In LSG melt, the buoyancy force necessary for pulling of bubbles toward top of the melt is

obtained when the size of the bubbles is small. The solubility of gas molecules inside lead silicate glass due to lower structure connectivity of the melt is high. This phenomenon and the higher rising rate of bubbles cause the bubbles spend lower time to grow.

The variation of mean size and standard deviation of bubbles in low heat treatment temperatures are high but their values are reduced by increasing of temperature. By comparing these results with the images of bubbles taken in different heat treatment times and temperatures (Fig. 6), it is observed that in lower time and temperatures the large size bubbles are present in companion with other ones. But by increasing heat treatment times and temperatures the large bubbles are removed from the melt and all bubbles have relatively finer size distribution. The variation of mean bubble size with time and temperature show that the mean bubble size is reduced by disappearing of larger bubbles in higher times.

Practical application. A useful practical experience was acquired for measurement of the volume, size and the number of gas bubbles inside liquids by measuring the dry, wet and floating weights of vessel without and with solidified melt. By using these data one can discus experimentally about the kinetic of bubble removing process. Determination of the mechanism and the kinetic of bubble removing from glass melt are important in glass industry. Bubble removing is affected by diffusion of gas molecules through the melt, dissolution of bubbles in melt or ascension of them to the surface and bursting in the surface of the melt. In soda-lime-silica glass melt chemically by addition of some additives the possibility of growth of large bubbles and dissolution of small bubbles or mechanically by mixing of the melt and charging gas to the melt, the bubble removing process are proceeded. It was obtained that in lead silicate glass melt ever a bubbly layer with any size of bubbles is formed on the surface of the melt which under that there was not any bubbles in the melt and dissolution of bubbles is not determining factor. It is obvious that it is not necessary to invest capital for preparing any bubble removing materials or equipment. In this study it was revealed that the main source of the gas molecules dissolved in the lead silicate glass melt and generated a huge number of bubbles come from the redox reaction of the lead element.

CONCLUSIONS

The transfer of oxygen molecules from the atmosphere through the large surface area of the powder during heating, facilitate the generation of the Pb_3O_4 by redox reaction below 550°C. In temperatures higher than that the reverse redox reaction creates oxygen molecules which in releasing from the glassy network prevented due to softening and sticking of LSG powders with each other. These oxygen molecules with the trapped air between the empty spaces of the powders dissolved in the viscous melt. By decreasing viscosity of the melt due to increasing of the temperature and reaching to super saturation the large amount of bubbles homogeneously are nucleated and grown in the whole area of the melt. By passing of time a bubbly layer forms at top of the LSG melt which by increasing time and temperature it is removed. Size and number of the bubbles depend on the time after liquefaction of the glasses. At $15 \le t \le 30$ min, the rate of diminution of the number of bubbles is much greater than at $30 \le t \le 45$ min. Enhancement of temperature results in reduction of the number and volume of the bubbles and thickness of glass layer between the bubbles. Average bubble size reduces with the glass temperature except at the first 15 min during which the mean bubble size increases. This only happens up to 1050°C, above which bubble-size decrease occurs.

REFERENCES

1. Pilon, L., Fedorov, A.G., Ramkrishna, D., and Viskanta, R., Bubble transport in three-dimensional laminar gravity-driven flowMathematical formulation, *J. Non-Cryst. Solids*, 2004, vol. 336, no. 2, pp. 71–83.
2. Pilon, L. and Viskanta, R., Bubble transport in three-dimensional laminar gravity-driven flow—Numerical results, *J. Non-Cryst. Solids*, 2004, vol. 336, no. 2, pp. 84–95.
3. Nemec, L. and Tonarova, V., Behavior of bubbles in glass melts under effect of the gravitational and centrifugal fields, *Ceram.-Silic.*, 2005, vol. 49, no. 3, pp. 162–169.
4. Nemec, L., Jebava, M., and Cincibusova, P., The removal of bubbles from glass melts in horizontal or vertical channels with different glass flow patterns, *Ceram.-Silic.*, 2006, vol. 50, no. 3, pp. 140–152.
5. Nemec, L., Refining in the glassmelting process, *J. Am. Ceram. Soc.*, 1977, vol. 60, nos. 910, pp. 436–440.
6. Nemec, L. and Ullrich, J., Calculations of interactions of gas bubbles with glass liquids containing sulfates, *J. Non-Cryst. Solids*, 1998, vol. 238, nos. 12, pp. 98–114.
7. Sycheva, G.A., Formation of the bubble structure in the $26Li_2O \cdot 74SiO_2$ glass, *Glass Phys. Chem.*, 2009, vol. 35, no. 3, pp. 267–273.
8. Kwak, H.-Y. and Kang, K.-M., Gaseous bubble nucleation under shear flow, *Int. J. Heat Mass Transfer*, 2009, vol. 52, nos. 2122, pp. 4929–4937.
9. Lensky, N.G., Niebo, R.W., Holloway, J.R., Lyakhovsky, V., and Navon, O., Bubble nucleation as a trigger for xenolith entrapment in mantle melts, *Earth Planet. Sci. Lett.*, 2006, vol. 245, nos. 12, pp. 278–288.
10. Jucha, R.B., Powers, D., Mcneil, T., Subramanian, R.S., and Cole, R., Bubble rise in glass-melts, *J. Am. Ceram. Soc.*, 1982, vol. 65, no. 6, pp. 289–292.
11. Kentish, S., Lee, J., Davidson, M., and Ashokkumar, M., The dissolution of a stationary spherical bubble beneath a flat plate, *Chem. Eng. Sci.*, 2006, vol. 61, no. 23, pp. 7697–7705.

12. Lillico, D.A., Babchin, A.J., Jossy, W.E., Sawatzky, R.P., and Yuan, J.Y., Gas bubble nucleation kinetics in a live heavy oil, *Colloids Surf., A*, 2001, vol. 192, pp. 25–38.
13. Sycheva, G.A., Influence of the presence of bubbles on the parameters of crystal nucleation in the $26Li_2O \cdot 74SiO_2$ glass, *Glass Phys. Chem.*, 2009, vol. 35, no. 6, pp. 602–612.
14. Fedorov, A.G. and Pilon, L., Glass foams: Formation, transport properties, and heat, mass, and radiation transfer, *J. Non-Cryst. Solids*, 2002, vol. 311, no. 2, pp. 154–173.
15. Kim, D.S., Dutton, B.C., Hrma, P.R., and Pilon, L., Effect of furnace atmosphere on E-glass foaming, *J. Non-Cryst. Solids*, 2006, vol. 352, nos. 50–51, pp. 5287–5295.
16. Hrma, P., Effect of heating rate on glass foaming: Transition to bulk foam, *J. Non-Cryst. Solids*, 2009, vol. 355, nos. 45, pp. 257–263.
17. Image J software: rsbweb.nih.gov/ij/.
18. Singer, F. and Singer, S.S., *Industrial Ceramics*, London: Chapman and Hall, 1971, p. 342.
19. Shelby, J.E., *Introduction to Glass Science and Technology*, London: Royal Society of Chemistry, 2005, 2nd ed., p. 150.
20. Steger, W.E., Landmesser, H., Boettcher, U., and Schubert, E.J., Infrared spectra of amorphous oxides, *Mol. J. Struct.*, 1990, vol. 217, no. 1, pp. 341–346.
21. Bray, P.J., Geissberger, A.E., Bucholtz, F., and Harris, I.A., Glass structure, *J. Non-Cryst. Solids*, 1982, vol. 52, nos. 1–3, pp. 4566.
22. Volf, M.B., *Chemical Approach to Glass, Glass Science, and Technology*, Amsterdam, The Netherlands: Elsevier, 1984, vol. 7, p. 443.
23. Rao, B.G., Sundar, H.G.K., and Rao, K.J., Investigations of glasses in the system $PbOPbF_2$, *J. Chem. Soc., Faraday Trans. 1*, 1984, vol. 80, no. 12, pp. 3491–3501.
24. Salagram, M., Krishna Prasad, V., and Subrahmanyam, K., IR and optical study of $PbO(2PbO \cdot PbO_2)$ glass containing a small amount of silica, *J. Alloys Compd.*, 2002, vol. 335, no. 1, pp. 228–232.
25. Norton, F.J., Permeation of gaseous oxygen through vitreous silica, *Nature* (London), 1961, vol. 191, p. 701.
26. Harper, C.A., *Handbook of Ceramics, Glasses, and Diamonds*, New York: McGraw-Hill, 2002, pp. 5.42–5.43.
27. Shelby, J.E., *Introduction to Glass Science and Technology*, London: Royal Society of Chemistry, 2005, 2nd ed., pp. 124–126.
28. Hornyak, E.J. and Weinberg, M.C., Velocity of a freely rising gas bubble in a sodalime silicate glass melt, *J. Am. Ceram. Soc.*, 1984, vol. 67, no. 11, pp. c244–c246.
29. Li, K.-W.K. and Schneider, A., Rise velocities of large bubbles in viscous Newtonian liquids, *J. Am. Ceram. Soc.*, 1995, vol. 76, no. 1, pp. 241–244.